

Nucleation times in the 2D Ising model

Kevin Brendel, G.T. Barkema and Henk van Beijeren

Theoretical Physics, Utrecht University, Leuvenlaan 4, 3584 CE Utrecht, the Netherlands

(Dated: March 22, 2019)

A theoretical framework is presented for the estimation of nucleation times in systems with Brownian type dynamics. This framework is applied to a prototype system: the two-dimensional Ising model with spin-flip dynamics in an external magnetic field. Direct simulation results for the nucleation times, spanning more than four orders of magnitude, are compared with theoretical predictions. There are no free parameters; all system properties required by the theory are determined by simulations in equilibrium systems. Theoretical and simulation values are found to agree in most cases within 20%.

I. INTRODUCTION

Nucleation, the process of escape from a metastable state via the spontaneous growth of a stable nucleus in a metastable surrounding, has been studied often before, and excellent books and reviews exist [1]. A prototype system to study nucleation phenomena is the well-known Ising model. Above the so-called critical temperature, in absence of an external magnetic field, up- and down-pointing spins are roughly equally abundant. Below the critical temperature, the system prefers to be in either of two states: one state with a positive magnetization in which most spins are pointing up, and one state with a negative magnetization. In the presence of an external field one of these states will become metastable, and will decay to the stable equilibrium state with a certain nucleation rate.

In an earlier article [2], we presented a theoretical framework to describe activated processes in systems with Brownian type dynamics. We then tested this framework in the study of magnetization reversal times in the two-dimensional Ising model. This first test-case was especially simple, since many properties of the transition state, i.e. the state with highest free energy on the trajectory from one free energy minimum to the other, were well-known. For instance, it is a state in which half the system has a positive, and the other half a negative magnetization, and these two regions are separated by a pair of interfaces which span the shorter dimension of the simulation cell.

Here, we apply this framework to nucleation phenomena. Starting in the metastable state in which most spins are anti-aligned with the external field, the system evolves via a transition state in which a droplet of spins aligns with the field, to the stable minimum in which most spins are aligned with the external field. This system is more complex than that of magnetization reversal in the absence of an external field: the size and shape of the critical droplet are not known a priori. Acharyya and Stauffer studied nucleation times in the two- three- and four-dimensional Ising model with external field, and found agreement with predictions of classical nucleation theory [3]. Here, we study the two-dimensional case in much more detail.

The organization of our manuscript is as follows. In section II, we describe the model that we study in detail. Next in section III, we outline the theoretical framework, based on our work on magnetization reversals, but extended to nucleation phenomena. We then apply this framework to our prototypical model —nucleation in the Ising model with spin-flip dynamics. In section IV we compare the theoretical predictions with high-accuracy computational results.

II. DETAILED DESCRIPTION OF THE MODEL

We consider the Ising model on a square lattice with lateral dimension L , periodic (helical) boundary conditions, and an external magnetic field h which favors downward-pointing spins, with the Hamiltonian

$$H = -J \sum_{\langle i,j \rangle} s_i s_j + h \sum_i s_i, \quad (1)$$

in which $s_i = \pm 1$ is the spin at site i , and J is the coupling constant. The summation runs over all pairs of nearest-neighbor sites; those of site i are $j = i \pm 1$ modulo N and $j = i \pm L$ modulo N , with $N = L^2$. The magnetization is defined as $M \equiv \sum_i s_i$; it can take values $M = -N, -N + 2, \dots, N$; all through this manuscript, we restrict ourselves to systems in which L is even. As a consequence, M takes only even values, and summations over a range of possible magnetizations only run over even numbers, with an increment of 2.

The system evolves in time according to single-spin-flip dynamics with Metropolis acceptance probabilities [4]. If C_i is the configuration after i proposed spin flips, a trial configuration C'_{i+1} is generated by flipping a single spin at a random site. This trial configuration is then either accepted ($C_{i+1} = C'_{i+1}$) or rejected ($C_{i+1} = C_i$); the acceptance probability is given by

$$P_a = \min [1, \exp(-\beta(E(C'_{i+1}) - E(C_i)))] , \quad (2)$$

in which $\beta = 1/(k_B T)$ with Boltzmann constant k_B and temperature T . The time scale is set such that in one unit of time, on average each spin is proposed to be flipped once. So in our system, in one unit of time we perform N Monte Carlo steps.

III. THEORETICAL FRAMEWORK

To study the behavior of nucleation times at temperatures below the critical one we may consider an ensemble of a large number of systems prepared in states with no large negative clusters present and study the rate at which one of the clusters in the system grows beyond the critical cluster size, after which the system is removed from the ensemble. The spin-flip dynamics described above may be represented by a master equation for the probability distribution $P(\mathbf{S})$ of finding a system in the state \mathbf{S} at time t . Due to the huge number of possible states this master equation cannot be solved analytically or even numerically for system sizes of practical interest. Therefore, as an approximation we assume that we may treat the clusters of negative spins in the system as being independent. In this approximation, the probability that none of the N_c clusters has grown beyond the critical size, is simply the N_c^{th} power of the probability that a single cluster has not grown beyond the critical size. The dynamics of a single cluster is then modeled by a master equation for the equilibrium probability $P(C, t)$ that this cluster contains C spins at time t :

$$\begin{aligned} \frac{dP(C, t)}{dt} = & \Gamma_{C, C+1}P(C+1, t) + \Gamma_{C, C-1}P(C-1, t) \\ & - (\Gamma_{C+1, C} + \Gamma_{C-1, C})P(C, t), \end{aligned} \quad (3)$$

with $\Gamma_{C', C}$ the transition rate from C to C' . In section IV B we describe how to estimate the transition rates $\Gamma_{C+1, C}$.

In order that the equilibrium distribution be a stationary solution of the master equation we impose the condition of detailed balance

$$\frac{\Gamma_{C+1, C}}{\Gamma_{C, C+1}} = \exp[\beta(F(C) - F(C+1))], \quad (4)$$

where, up to a constant, $\beta F(C) = -\ln P_{eq}(C)$, with $P_{eq}(C)$ the equilibrium probability of cluster size C .

The long-time nucleation rate as predicted by the master equation (3) follows as the largest eigenvalue (with a minus sign) of this equation, supplemented with an absorbing boundary at $C = A$. Here A is an integer larger than the critical cluster size C_x , chosen such that $P_{eq}(A) \gg P_{eq}(C_x)$, and clusters with size A are almost certain to nucleate. The absorbing boundary condition is implemented by setting $\Gamma_{A-1, A}$ equal to zero.

The largest eigenvalue $-\nu$ of $\Gamma_{C, C'}$ in Eq. (3), as well as the corresponding eigenvector $P_0(C)$, may be found by requiring that the net current away from cluster size C assumes the value $\nu P_0(C)$. Using conservation of probability one easily checks that this may be expressed as

$$\begin{aligned} j_{C+1, C} & \equiv \Gamma_{C+1, C}P_0(C) - \Gamma_{C, C+1}P_0(C+1) \\ & = \nu \sum_{c \leq C} P_0(c), \end{aligned} \quad (5)$$

$$\nu = \frac{\Gamma_{A, A-1}P_0(A-1)}{\sum_{c \leq A-1} P_0(c)}, \quad (6)$$

where $j_{C+1, C}$ is defined as the net current flowing from C to $C+1$. This current may be approximated by

$$\begin{aligned} j_{C+1, C} & = \nu \frac{\sum_{c=1}^C \exp[-\beta F(c)]}{\sum_{c=1}^{C_x} \exp[-\beta F(c)]}, \quad c \leq C_x \\ j_{C+1, C} & = \nu, \quad c \geq C_x \end{aligned} \quad (7)$$

because the sum on the right hand side of Eq. (5) is dominated by the terms with small c -values, for which $P_0(c)$ is approximately proportional to $\exp[-\beta F(c)]$. This may be checked in hindsight against the solution obtained. With this approximation the equation may be solved recursively for $P_0(c)$ in terms of $P_0(A-1)$ for $c = A-2, A-3, \dots$, with the result

$$\frac{P_0(c)}{P_0(A-1)} = \frac{\Gamma_{A, A-1}}{\nu} \sum_{m=c}^{A-1} j_{m+1, m} \frac{\exp[\beta(F(m) - F(c))]}{\Gamma_{m+1, m}}. \quad (8)$$

Since the sum over m is dominated by values close to or larger than the critical cluster size, for which $j_{m+1, m}$ is approximately equal to ν , we may replace Eq. (8) by

$$\frac{P_0(c)}{P_0(A-1)} = \Gamma_{A, A-1} \sum_{m=c}^{A-1} \frac{\exp[\beta(F(m) - F(c))]}{\Gamma_{m+1, m}}. \quad (9)$$

Now substituting this into Eq. (6) we arrive at the result

$$\nu = \left(\sum_{m=1}^{A-1} \frac{\exp[\beta F(m)]}{\Gamma_{m+1, m}} \sum_{c=1}^{C_x} \exp[-\beta F(c)] \right)^{-1}, \quad (10)$$

where we have used the fact that the sum over c is dominated by small values of c to extend the sum over m to $m=1$. The result in Eq. (10) is well-known. It is usually derived by considering a state with a stationary current in which mass is inserted at a constant rate on one side (e.g. at $C=0$ in our case) and taken out as soon as it reaches the absorbing boundary (see e.g. [5], section IV E). In that case the replacement of $j_{m+1, m}$ by a constant is exact.

One may give an even more accurate representation of the long time behavior of $P(C, t)$ for arbitrary initial distributions $P(C, 0)$ that are concentrated near the origin, by writing it in the form

$$P(C, t) = kP_0(C) \exp[-\nu t] \text{ for } t \rightarrow \infty, \quad (11)$$

where k is a constant which represents the overlap between $P(C, 0)$ and $P_0(C)$. This gives for the probability $S(t)$ that the system has not yet nucleated at time t

$$S(t) = \sum_{C=1}^{A-1} P(C, t) = \exp[-\nu(t - t_d)] \text{ for } t \rightarrow \infty, \quad (12)$$

where t_d is called the delay time. The value of t_d may be obtained from the projection of the initial cluster size

distribution $P(C, t)$ onto the most slowly decaying eigenfunction of the master equation, (3). This eigenfunction was given (with a different normalization) in Eq. (8):

$$\begin{aligned} \psi^r(n) &\equiv \frac{\nu}{P_0(A-1)\Gamma_{A,A-1}} P_0(n) \\ &= \sum_{m=n}^{A-1} j_{m+1,m} \frac{\exp[\beta(F(m) - F(n))]}{\Gamma_{m+1,m}}. \end{aligned} \quad (13)$$

with $j_{m+1,m}$ given in Eq. (7). As a consequence of the condition of detailed balance, Eq. (4), the corresponding left eigenvector is obtained by multiplying $\psi^r(n)$ by $\exp[\beta F(n)]$, or

$$\tilde{\psi}^l(n) = \sum_{m=n}^{A-1} j_{m+1,m} \frac{\exp[\beta F(m)]}{\Gamma_{m+1,m}}. \quad (14)$$

Notice that for small values of n this is virtually independent of n , because only the largest m -values give important contributions to the sum. Using the proper normalization of the leading eigenfunction, and approximating $P(C, 0)$ by $\delta_{C,1}$, one now finds immediately that t_d follows from

$$\exp[\nu t_d] = \frac{\tilde{\psi}^l(1) \sum_{n=1}^{A-1} \left(\exp[-\beta F(n)] \tilde{\psi}^l(n) \right)}{\sum_{n=1}^{A-1} \left(\exp[-\beta F(n)] \left(\tilde{\psi}^l(n) \right)^2 \right)}. \quad (15)$$

Now, by subtracting unity on both sides, dividing by ν , approximating sums over m from n to $A-1$ by sums from 1 to $A-1$, where appropriate, and using Eq. (7) to replace $j_{m+1,m}$ appearing in the left-hand sum of the nominator, one obtains

$$t_d = \frac{\sum_{n=1}^{A-1} \sum_{m=1}^{n-1} \left(\frac{W(n)}{\Gamma_{m+1,m} W(m)} \sum_{k=1}^{\min[m, C_x]} W(k) \right) \tilde{\psi}^l(n)}{\sum_{n=1}^{A-1} \left(W(n) \tilde{\psi}^l(n) \right)}, \quad (16)$$

with $W(n) \equiv \exp(-\beta F(n))$.

IV. SIMULATIONS AND RESULTS

If one wants to apply the above theoretical framework to nucleation times in the Ising model, the two ingredients required are: (i) the equilibrium probability $P_{eq}(C)$ to find a cluster of size C ; and (ii) the transition rates $\Gamma_{C',C}$ from cluster size C to C' . We obtain these two ingredients via two different computational approaches. In all our simulations, we use a technique known as multi-spin coding [6], which enables us to reach long simulation times and thus good statistics.

A. free energy landscape

We measure the distribution of cluster sizes for various values of β and h , in a system with 64×64 spins. We are actually only interested in the distribution of clusters smaller than a certain size A , which was discussed in section III. Therefore we define a cut-off cluster size C_{max} , which is typically chosen to be 300. We modify our algorithm in the following way: starting with a configuration C_i we perform a fixed number M of Monte Carlo steps, and measure the sizes of all the clusters of down-spins in the system. If there is a cluster with more than C_{max} spins we reject the new configuration, and choose $C_{i+1} = C_i$. Otherwise we accept the new configuration as our C_{i+1} . In both cases we add the distribution of cluster sizes in C_{i+1} to the histogram. Finally we find the free energy $F(C)$ from

$$\beta F(C) = -\ln \frac{N(C)}{\sum_{C \leq C_{max}} N(C)}, \quad (17)$$

where $N(C)$ is the average number of clusters of size C in the histogram.

If C_{max} is chosen too large, the various clusters in the system influence each other. In particular, excluded volume effects around large clusters suppress bigger clusters in the metastable state more than smaller ones. As a consequence the distribution of cluster sizes depends on C_{max} . To determine whether a certain value of C_{max} is allowed, we check that for small clusters the free energy curve coincides with the same curve, obtained with a lower value for C_{max} .

Figure 1 shows our measurements for the free energy according to Eq. (17) as a function of island size, for some combinations of temperature and external field.

For large circular islands, classical nucleation theory can be used. The free energy is then approximated by the Becker-Döring expression [7]

$$F(C) \approx F_0 + 2\sigma\sqrt{\pi C} - 2hC, \quad (18)$$

where F_0 is some constant, σ the excess free energy of the interface per unit length, and h the strength of the external field. We fitted F_0 and σ to the data in figure 1, and added the corresponding curves as lines in the same figure. As expected, the measurements are well fitted by the curves, as long as the island size is not too small.

The surface tensions obtained in this way are larger than those given by the Onsager expression [8]

$$\sigma = 2J + \beta^{-1} \ln \tanh \beta J, \quad (19)$$

which is valid for long horizontal or vertical interfaces, and zero external field (see figure 2). We will address this issue in a separate paper [9].

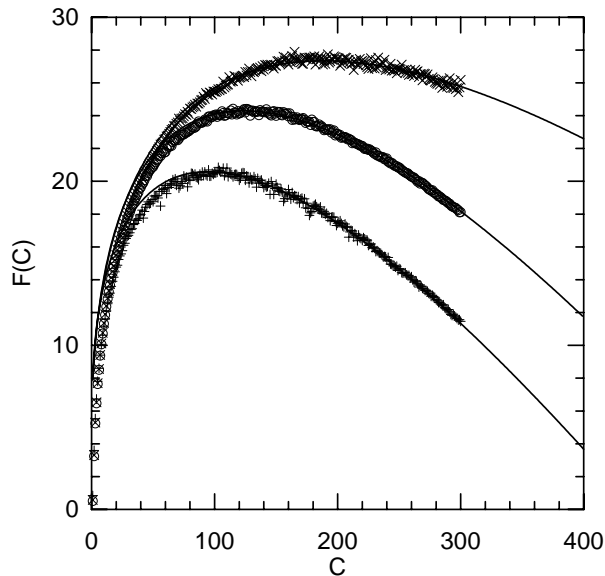


FIG. 1: Free energy as a function of cluster size in the 64×64 system at $\beta J = 0.58$ and $h = 0.08$ (\circ), $\beta J = 0.53$ and $h = 0.08$ ($+$), and $\beta J = 0.56$ and $h = 0.06$ (\times). In the simulations, C assumes integer values ≥ 1 . The lines represent the Becker-Döring expression Eq. (18), with fitted values for σ .

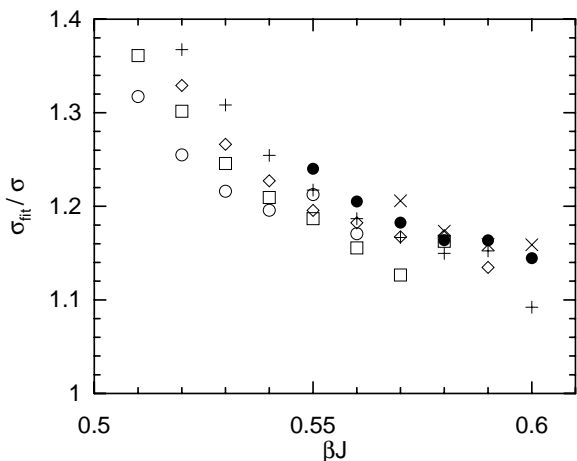


FIG. 2: Surface tension obtained by fitting the free energy curve, divided by the values given in Eq. (19), as a function of βJ . Different symbols denote different strengths of the external field: $h = 0.05$ (\circ), $h = 0.06$ (\square), $h = 0.07$ (\diamond), $h = 0.08$ ($+$), $h = 0.09$ (\bullet) and $h = 0.10$ (\times).

B. interface diffusion coefficient

The second ingredient in the theoretical framework in section III is the rate $\Gamma_{C+1,C}$ of cluster growth. To estimate this rate we study the diffusion of a single interface in a system with anti-periodic boundary conditions in the absence of an external field, as described in [2]. The location of the interface is obtained from the magnetization

M . The diffusion coefficient D is defined as:

$$D = \lim_{t \rightarrow \infty} \left[\frac{\langle (M(t) - M(0))^2 \rangle}{2t} \right]. \quad (20)$$

This diffusion coefficient is, to a good approximation, found to be linear in the length of the interface B :

$$D(B, L, \beta J) = g(\beta J)B + c, \quad (21)$$

with the constant c very close to zero. The results for $g(\beta, J)$ for various temperatures are plotted in figure 3.

To arrive at an estimate for the rate $\Gamma_{C+1,C}$ for cluster growth and shrinkage, we assume that the diffusion coefficient neither depends on the external field nor on the shape of the interface (straight or circular), but only on the length of the cluster boundary, which in our case we set to $2\sqrt{\pi C}$. For large clusters this should be a very good approximation. From Eqs. (10) and (16) we see that the contributions from small clusters to the expressions for ν and t_d are almost insignificant, and inaccurate estimates of the cluster boundary length for those clusters is not very important. This then gives rise to a jump rate

$$\Gamma_{C+1,C} = \frac{g(\beta J)}{4} 2\sqrt{\pi C}. \quad (22)$$

The factor 4 arises because the jumps in magnetization go by units of 2. Notice that instead of identifying $\Gamma_{C+1,C}$ through D we could have taken $\Gamma_{C,C+1}$ just as well. Due to the free energy profile these quantities are not identical, though never much different, but fortunately, for C -values close to the free energy maximum, which are weighted most strongly, their difference becomes very small. In addition there will be some compensating effects, because for $C \geq C_x$ one has $\Gamma_{C+1,C} > \Gamma_{C,C+1}$ whereas for $C < C_x$ this is just the other way around.

C. nucleation rates

To measure the long-time nucleation rates, we first bring the system into equilibrium. At time $t = 0$, we then reverse all the spins so that the system is near its metastable equilibrium. We measure the time the system needs to reach the magnetization corresponding to the stable equilibrium. We make a histogram of all the measured times.

Figure 4 shows that at long times the decay function $f(t)$ behaves as $f(t) \sim \exp(-\nu_s t)$. Here, we focus on the long-time behavior, and are specifically interested in the escape rate ν_s . We obtain this quantity via a fitting procedure, in which we ignore the data up to a time t_0 , chosen such that $f(t)$ shows exponential time behavior for $t > t_0$. Then we determine the time t' at which half of the remaining events have taken place. We then obtain the relaxation time $\tau \equiv \nu_s^{-1}$ from $\tau = (t' - t_0) / \ln(2)$. Instead we could have made a linear fit of all the data points beyond t_0 , but this makes no significant difference. Table I gives the measured relaxation times τ_1 . In

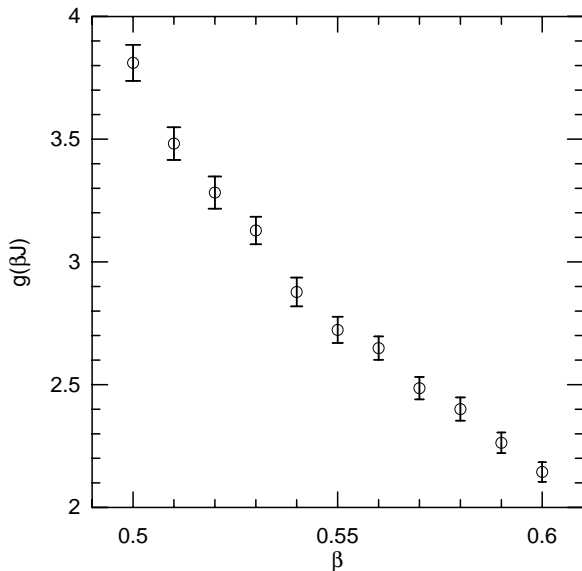


FIG. 3: Monte Carlo measurements of the diffusion coefficient per interface length $g(\beta J)$, as a function of inverse temperature βJ .

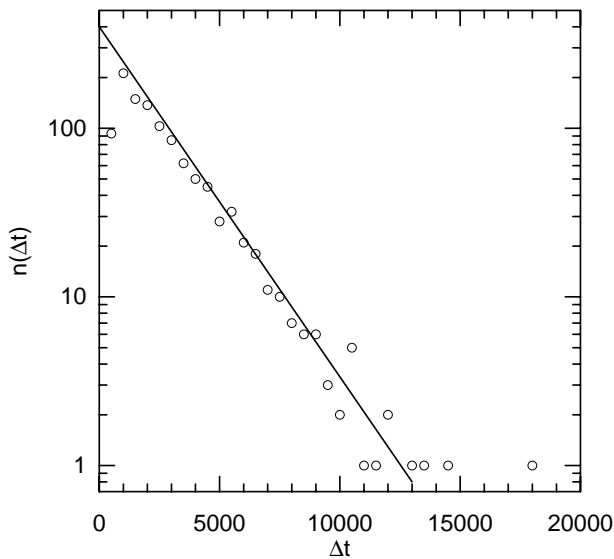


FIG. 4: Histogram of the time Δt elapsed before nucleation occurs, at inverse temperature $\beta J = 0.54$ and external field strength $h = 0.08$, in a system with 64×64 sites. The straight line is a fit, given by $n(\Delta t) \sim \exp(\Delta t/1990)$.

the same table, we also report the estimated relaxation times $\tau_2 = (\langle N_c \rangle \nu)^{-1}$ with ν as obtained in Eq. (10) and $\langle N_c \rangle \equiv \sum_{C=1}^A N(C)$ the average number of clusters in the system. Finally we also give the ratio τ_2/τ_1 . The table shows that, while the relaxation times span more than four decades in time, the estimated and measured relaxation times agree mostly within 20%.

D. short-time behavior

Besides the long-time exponential behavior of the nucleation probability, we also study the deviation from this behavior at short times. To do this, the master equation (3) for the time evolution of one cluster is solved numerically, with the initial condition that the cluster consists of a single spin:

$$P(C, 0) = \delta_{C,1}. \quad (23)$$

We then compute the cumulative probability distribution $P_{nuc}(1, t)$ that the cluster has grown beyond a certain size C_{max} during time t . The corresponding probability distribution for the nucleation of one of N_c statistically independent clusters at C_{max} , at time t , is given by

$$1 - P_{nuc}(N_c, t) = (1 - P_{nuc}(1, t))^{N_c}. \quad (24)$$

The quantity $P_{nuc}(N_c, t)$ should be equal to the cumulative distribution of nucleation times, if we use as a definition of nucleation the first occurrence of a cluster of C_{max} spins anywhere in the system.

We have compared this result with the results of direct simulations, for $\beta = 0.54$ and $h = 0.08$. We did this for three different system sizes: 32×32 , 64×64 , and 128×128 . In all cases the starting configuration was a system with zero magnetization. Within a few time steps this develops into a quasi-equilibrium distribution as far as the distribution of small cluster sizes is concerned, so for the present system sizes the fact that we started from clusters of size zero rather than unity makes no difference. Figure 5 shows the results. Here, we used for N_c the mean number of clusters in the system as obtained from the same simulations that were used to obtain the free energy as a function of cluster size.

The asymptotic slopes of the curves in the top panel of figure 5 correspond to the nucleation rates. The times at which straight-line fits to these curves cross $1 - P_{nuc} = 1$ correspond to the waiting times t_d . There is excellent agreement between the direct simulations and the parameter-free theoretical framework: The theoretical prediction obtained with Eq. (16) is $t_d = 234$ MC time units, while the fits vary between $t_d = 228$ and 239 MC time units. Also the behavior at short times is well described by the theoretical framework, as is evidenced in the bottom panel of figure 5. The agreement at late times was discussed above.

V. DISCUSSION

In this paper we showed that for two dimensional Ising models with spin-flip dynamics Becker-Döring theory provides an excellent description of nucleation time distributions, provided a realistic description is used for the free energy of the growing droplets. We determined this free energy from cluster size distributions in equilibrium Monte Carlo simulations and found it may be fitted well by the Becker-Döring expression, provided one

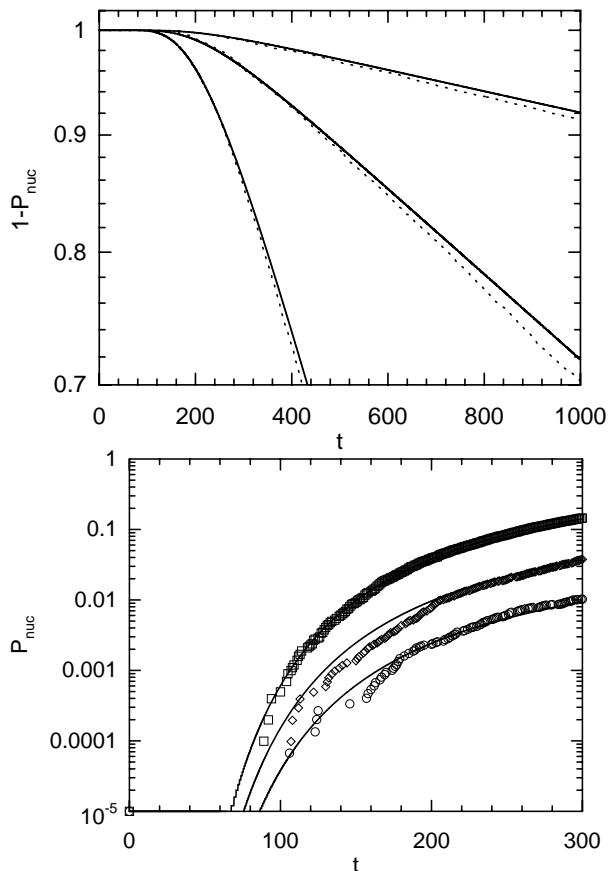


FIG. 5: $1 - P_{nuc}(t)$ obtained from the time evolution of one cluster (solid lines) according to the master equation (3) combined with Eq. (24), and by direct simulation of systems with 32×32 , 64×64 , and 128×128 spins (the dotted lines) at $\beta J = 0.54$ and $h = 0.08$. In both cases, the highest of the three curves corresponds to the smallest system, and the lowest one to the largest system. The lower plot shows the same data, but focuses on short times.

uses surface tensions that are 10 to 20% higher than the surface tension of a bulk interface at zero field. Similar conclusions were reached by Auer and Frenkel[10] in their studies of crystal nucleation in colloidal hard sphere systems. They also determined cluster free energies by monitoring the frequency of occurrence of clusters of a given size. Like we they could fit the resulting curves quite well by a Becker-Döring expression with an effective surface tension that exceeds the bulk surface tension by in their case 20 to 40%.

A point one may question is whether the assumption of independent noninteracting clusters holds even for clusters of small size. This may indeed be doubted, but fortunately, at least for the asymptotic nucleation frequency $\langle \nu N_c \rangle$ this is not really relevant. One may choose to define as clusters only those clusters that have a size $c \geq m_0$, with m_0 chosen such that clusters of this size already are very rare, but still $\exp(\beta F(m_0)) \ll \exp(\beta F(C_x))$.

From Eqs. (10) and (17) it then follows that

$$\nu_{m_0} = \frac{\sum_{c=1}^{C_x} N_c}{\sum_{c=m_0}^{C_x} N_c} \nu,$$

since the terms with $m < m_0$ in the first sum in (10) basically do not contribute. As a consequence of this the asymptotic nucleation rate in the system is independent of the choice of m_0 .

For the short-time nucleation rate the free energy of small clusters is also important, especially if one starts from a state of zero magnetization. However, if one starts from a quasi-equilibrium distribution representing the state after a sudden reversal of the magnetic field, the short time behavior will be dominated by clusters that were fairly large to start with and again Eq. (17) may be trusted. In [11] Van Beijeren gave explicit expressions for the short-time behavior, which may be used if the latter is well approximated by a diffusion equation in an external potential. In the present case these cannot be used, since on the relevant time scales the hopping process between neighboring cluster sizes is not well-approximated by a diffusion process. And since the hopping rates depend on cluster size no analytic expressions for the short-time behavior are available. But the numerical solution of the master equation (3) gives a very good agreement with the results from our Monte Carlo simulation of the nucleation process, as was shown in Fig. 5.

Besides the free energy as a function of cluster size our calculations require the transition rates $\Gamma_{C,C\pm 1}$ between neighboring values of the cluster size. These we estimated by setting them proportional to the mean circumference of a cluster, determining the proportionality constant from the simulated mobility of a straight interface in cylindrical geometry and imposing the detailed balance condition (4).

In our estimations we have been using a number of assumptions, whose validity is not guaranteed under all conditions:

- Strong fields should modify the diffusion coefficient; this effect is neglected. The freedom to modify the field strength within the metastable region is limited though, and long nucleation times, as seen mostly in real experiments, require weak fields.
- The diffusion coefficient is assumed to be determined by the size of the cluster alone, and is calculated on the assumption that this shape is strictly spherical. This requires that the temperature is not too low, because at very low temperatures the equilibrium shape of the cluster is squarish rather than circular [12]. On the other hand the temperature should not be too close to the critical temperature for shape fluctuations to be reasonably small. To some extent these fluctuations are taken into account, since our calculation of the diffusion coefficient is done for a fluctuating interface around a cylinder. But it is by no means certain that the

fluctuations of a circular interface are in all aspects comparable to those of the interface around the cylinder.

- It may happen that an island splits up or that two islands merge, corresponding in our theoretical framework to non-zero transition rates $\Gamma_{C,C+i}$ and $\Gamma_{C+i,C}$ with $i > 1$. This effect also is partly accounted for through the numerical determination of the diffusion constant on a cylinder, but especially for larger islands the difference in geometry may cause additional effects. However, these will only become important in systems that contain a sizable density of islands of spins aligned with the external field. Hence, also this approximation can be trusted least near the critical point.
- No memory effects are accounted for explicitly. For spin-flip dynamics memory effects will chiefly be due to the influence of shape fluctuations on the transition rates. Since shape fluctuations on larger length scales will decay only slowly, these may be fairly long lasting effects. Again, our way of determining the diffusion coefficient will take many of these effects into account implicitly, but memory effects involving large shape fluctuations may be different for the present cluster geometry. For magnetization conserving dynamics (consisting e.g.

of local spin exchanges) much stronger memory effects exist due e.g. to the effect that a spin that is released from a large cluster has high probability of reattaching to it soon.

Under conditions in which the effects above are negligible, our theoretical framework is able to estimate nucleation rates with an accuracy in the range of 20%. The small systematic overestimation by about 10% of the nucleation time by theory may have several causes. The radius of a cluster will be slightly larger than our estimate because especially a large cluster will typically contain a few holes in its interior. But in the investigated range of temperatures this should not amount to a correction of more than 3%. The assumption that the diffusion coefficient is independent of the orientation of the interface also may be not entirely correct. At low temperatures certainly a diagonal interface is much more mobile than a straight one, but at the present fairly elevated temperatures one would not expect this effect to be large. Further there could be effects from the possibility of cluster splittings and mergings, though some of these certainly are accounted for through the numerical determination of the diffusion constant on a cylinder.

We are currently extending our investigations to two-dimensional Ising systems with magnetization-conserving dynamics as well as to three-dimensional Ising systems.

-
- [1] P. G. Debenedetti, “*Metastable Liquids*”, (Princeton University Press, Princeton, 1996).
- [2] K. Brendel, G. T. Barkema and H. van Beijeren, *Phys. Rev. E* **67**, 026119 (2003).
- [3] M. Acharyya and D. Stauffer, *European Physical Journal B* **5**, 571 (1998).
- [4] N. Metropolis, A. W. Rosenbluth, M. N. Rosenbluth, A. H. Teller, and E. Teller, *J. Chem. Phys.* **21**, 1087 (1953).
- [5] P. Hänggi, P. Talkner and M. Borkovec, *Rev. Mod. Phys.* **62**, 251 (1990).
- [6] M. E. J. Newman and G. T. Barkema, “*Monte Carlo Methods in Statistical Physics*”, Oxford University Press, Oxford, 1999.
- [7] R. Becker and D. Döring, *Annalen der Physik* **5**, 24 (1935).
- [8] L. Onsager *Phys. Rev.* **65**, 117 (1944).
- [9] H. van Beijeren, G.T. Barkema and K. Brendel, to be published.
- [10] S. Auer and D. Frenkel, *Nature* **409**, 1020 (2001).
- [11] H. van Beijeren, *J. Stat. Phys.* **110**, 1397 (2003).
- [12] J. E. Avron, H. van Beijeren, L. S. Schulman and R. K. P. Zia, *J. Phys.* **A15**, L81 (1982).

TABLE I: Measured values (τ_1) and estimated values (τ_2) for the nucleation times in the 64×64 system.

βJ	H	τ_1	τ_2	τ_2/τ_1
0.51	0.04	$1.83 \cdot 10^4$	$2.26 \cdot 10^4$	1.234
0.51	0.05	$3.35 \cdot 10^3$	$3.84 \cdot 10^3$	1.146
0.51	0.06	$9.84 \cdot 10^2$	$1.14 \cdot 10^3$	1.163
0.52	0.04	$1.07 \cdot 10^5$	$1.09 \cdot 10^5$	1.019
0.52	0.05	$1.13 \cdot 10^4$	$1.31 \cdot 10^4$	1.153
0.52	0.06	$2.84 \cdot 10^3$	$3.57 \cdot 10^3$	1.257
0.52	0.07	$8.51 \cdot 10^2$	$1.09 \cdot 10^3$	1.276
0.52	0.08	$3.96 \cdot 10^2$	$4.49 \cdot 10^2$	1.134
0.53	0.05	$4.15 \cdot 10^4$	$4.79 \cdot 10^4$	1.153
0.53	0.06	$8.94 \cdot 10^3$	$9.47 \cdot 10^3$	1.059
0.53	0.07	$2.31 \cdot 10^3$	$2.57 \cdot 10^3$	1.111
0.53	0.08	$8.98 \cdot 10^2$	$9.59 \cdot 10^2$	1.068
0.54	0.05	$1.73 \cdot 10^5$	$2.13 \cdot 10^5$	1.228
0.54	0.06	$2.90 \cdot 10^4$	$3.11 \cdot 10^4$	1.071
0.54	0.07	$6.69 \cdot 10^3$	$7.27 \cdot 10^3$	1.087
0.54	0.08	$2.17 \cdot 10^3$	$2.32 \cdot 10^3$	1.068
0.55	0.05	$8.03 \cdot 10^5$	$1.13 \cdot 10^6$	1.410
0.55	0.06	$9.57 \cdot 10^4$	$1.08 \cdot 10^5$	1.126
0.55	0.07	$1.97 \cdot 10^4$	$2.08 \cdot 10^4$	1.054
0.55	0.08	$5.60 \cdot 10^3$	$5.98 \cdot 10^3$	1.070
0.55	0.09	$2.05 \cdot 10^3$	$2.17 \cdot 10^3$	1.058
0.56	0.05	$4.02 \cdot 10^6$	$4.59 \cdot 10^6$	1.140
0.56	0.06	$3.78 \cdot 10^5$	$4.17 \cdot 10^5$	1.103
0.56	0.07	$5.81 \cdot 10^4$	$6.44 \cdot 10^4$	1.109
0.56	0.08	$1.48 \cdot 10^4$	$1.57 \cdot 10^4$	1.058
0.56	0.09	$4.92 \cdot 10^3$	$5.11 \cdot 10^3$	1.038
0.57	0.06	$1.47 \cdot 10^6$	$1.36 \cdot 10^6$	0.927
0.57	0.07	$1.84 \cdot 10^5$	$1.98 \cdot 10^5$	1.080
0.57	0.08	$4.14 \cdot 10^4$	$4.40 \cdot 10^4$	1.062
0.57	0.09	$1.24 \cdot 10^4$	$1.24 \cdot 10^4$	1.000
0.57	0.10	$4.02 \cdot 10^3$	$4.53 \cdot 10^3$	1.128
0.58	0.06	$5.80 \cdot 10^6$	$6.60 \cdot 10^6$	1.139
0.58	0.07	$6.18 \cdot 10^5$	$5.72 \cdot 10^5$	0.926
0.58	0.08	$1.10 \cdot 10^5$	$1.26 \cdot 10^5$	1.143
0.58	0.09	$3.06 \cdot 10^4$	$3.11 \cdot 10^4$	1.015
0.58	0.10	$1.13 \cdot 10^4$	$1.06 \cdot 10^4$	0.938
0.59	0.07	$2.25 \cdot 10^6$	$2.48 \cdot 10^6$	1.104
0.59	0.08	$3.49 \cdot 10^5$	$4.22 \cdot 10^5$	1.209
0.59	0.09	$8.47 \cdot 10^4$	$8.36 \cdot 10^4$	0.987
0.59	0.10	$2.31 \cdot 10^4$	$2.47 \cdot 10^4$	1.068
0.60	0.08	$1.04 \cdot 10^6$	$1.19 \cdot 10^6$	1.145
0.60	0.09	$2.05 \cdot 10^5$	$2.52 \cdot 10^5$	1.229
0.60	0.10	$5.81 \cdot 10^4$	$6.72 \cdot 10^4$	1.156